A Contribution to Nyquist-Rate ADC Modeling - Detailed Algorithm Description

Jan ŽIDEK[1], *Ondřej ŠUBRT*[1,2], *Milan VALENTA*[1], *Pravoslav MARTINEK*[1]

[1]Faculty of Electrical Engineering Czech Technical University in Prague, Technická 2, 166 27 Prague 6, Czech Republic,
[2]ASICentrum s.r.o., Novodvorská 994, 142 21 Prague 4, Czech Republic

zidekja3@fel.cvut.cz, ondrej.subrt@asicentrum.cz, valenm1@fel.cvut.cz, martinek@fel.cvut.cz

Abstract. *In this article, the innovative ADC modeling algorithm is described. It is well suitable for Nyquist-rate ADC error back annotation. This algorithm is the next step of building a support tool for IC design engineers. The inspiration for us was the work [2]. Here, the ADC behavior is divided into HCF (High Code Frequency) and LCF (Low Code Frequency) separated independent parts. This paper is based on the same concept but the model coefficients are estimated in a different way only from INL data. The HCF order recognition part was newly added as well. Thanks to that the HCF coefficients number is lower in comparison with the original Grimaldi's work (especially for converters with low ratio between HCF and "random" part of INL). Modeling results are demonstrated on a real data set measured by ASICentrum on charge-redistribution type SAR ADC chip. Results are shown not only by coefficient values but also by the Model Coverage metrics. Model limitations are also discussed.*

Keywords

Analog-digital integrated circuits, Modeling, Order detection, HCF, LCF.

1. Introduction

1.1 State of the Art

Modeling of electronic parts and circuits is usually the first step in general error mechanisms analysis. Nowadays, it is very important to model analog as well as mixed-signal aspects of the integrated circuits; this trend is most apparent in Data Converters which are typical representatives. Two of basic parameters specifying the performance of A/D converters are Integral (INL) and Differential (DNL) Non-Linearity [1]. Several ADC INL and DNL modeling methods are discussed in recent articles. For example, time-delay power series in [3]; polynomial, Chebyshev polynomial and Fourier series approximation in [4]; and neural network based model in [5]. In our opinion, the nearest to ADC circuit representation is the system of High Code Frequency (HCF) and Low Code Frequency (LCF) functions. Bases of this model type are described in the very often cited article [2]. The authors specified the Unified ADC Error Model in it. This model is described by two independent functions, HCF and LCF. The paper also describes how to obtain LCF and HCF coefficients. Three different methods for LCF determination are tried (Least Mean Squares (LMS), Lagrange polynomial and Spline curves). There are no methods used by the other authors except the LMS extraction of the LCF polynomial coefficients. The HCF is measured from peaks in DNL.

This idea is further developed in [6]. Transfer function key data points positions are investigated. The measurement of these points is only needed for the precise model assembling. It is also shown that the modeling only by LCF needs a high order of the polynomial (about 25 coefficients), whereas the combination of LCF and HCF rapidly reduces the total amount of parameters (not more than 12 is needed). And LCF order increasing over ten leads to LCF and HCF independence elimination.

The LCF and HCF input signal frequency dependencies are observed in [7]. In the article, the method of decomposing LCF into frequency dependent and independent part is described. This idea is further developed and utilized in [8] where it is used for the ADC error post correction.

This article refers to previous work of our team [9] and [10].

1.2 HCF and LCF Model Description

We would like to clarify some key terms used in the following text by the short summary of Grimaldi's "Unified error model", which is deeply described in the already mentioned paper [2]. Continual pressure on power and area consumption of integrated circuits leads to preference of algorithmic ADCs in a wide range of applications. This type of converters has a typical static error characteristics. Especially INL and DNL curve has a multi-periodical shape. This well known behavior is given by the superposition principle of individual binary weights error. INL discontinuities occur

at the code interval key points (half, quarters, eighths, ...). It is obvious that the approximation (modeling) has to be done by a piecewise function set. The Rademacher's functions [11] are chosen by Grimaldi's team as base for modeling of peaks in DNL and discontinuities in INL subsequently. The Equations (4)-(3) are adopted from [2] and they have been changed to our notation. The Equation (4) expresses meaning of LCF coefficients. The Equations (1), (3) denote Rademacher functions, HCF mathematical expression, respectively.

$$RAD(n,C) = sign\left(sin\left(\frac{2^n \pi C}{N}\right)\right). \quad (1)$$

$$\Delta RAD(n,C) = \begin{cases} 1 & \text{if } RAD(n,C) - RAD(n,C-1) \neq 0, \\ 0 & \text{else,} \end{cases} \quad (2)$$

$$DNL_{HCF}(C) = \sum_{n=1}^{ORDER} H_n \Delta RAD(n,C). \quad (3)$$

The n in these equations is the order of the function and C stands for code value. The equation 3 represents the superposition of Rademacher's functions. It is an HCF part of the "Unified error model". The LCF part represents slow (as function of code) changes of the INL. The most important static parameters captured by the LCF are offset and gain error but the LCF is at least a function of the 4th order, so it holds other errors as well.

$$LCF(C) = L_0 + L_1 C + L_2 C^2 + L_3 C^3 + L_4 C^4. \quad (4)$$

This paper contains three parts. The first one describes the whole process of obtaining LCF and HCF coefficients. INL data modeling of a real SAR converter is shown in the second part and a conclusion finalizes the article.

2. Our Algorithm Description

The whole algorithm can be separated into four parts. Their purpose is as follows:

1. Finding the order of the HCF approximation,
2. Interpolation of INL by linear functions,
3. LCF acquisition from INL_{approx},
4. HCF coefficients calculation.

In the first and the second part of the algorithm the source INL data is approximated by a piecewise function (INL_{approx}). The third and fourth parts fit the ADC model to this function and extract model coefficients.

2.1 HCF Order Finding

The first part of the whole algorithm finds the highest meaningful order of HCF model fraction. Here, "meaningful" denotes the fact that by increasing the approximation order, the error is not further significantly decreased. This is shown in the flowchart in Fig. 1. There are two acronyms which should be defined. POINTSPRE stands for the number of investigated PREceding POINTS to the INL key point. ORDER is a variable which holds and at the end returns the found order of HCF function.

The process is easy to understand. ORDER and POINTSPRE values are set at the algorithm start. Subsequently, the algorithm enters the loop statement, where the ORDER value is incremented and INL data is tested in significant points. Mid-code INL value is taken for the first run (i.e., it corresponds to the testing for the first order). This value is then compared with POINTSPRE number of preceding values. If all the mentioned values of the preceding INL data are lower or all higher than the mid-code one, the algorithm enters the testing for the next order.

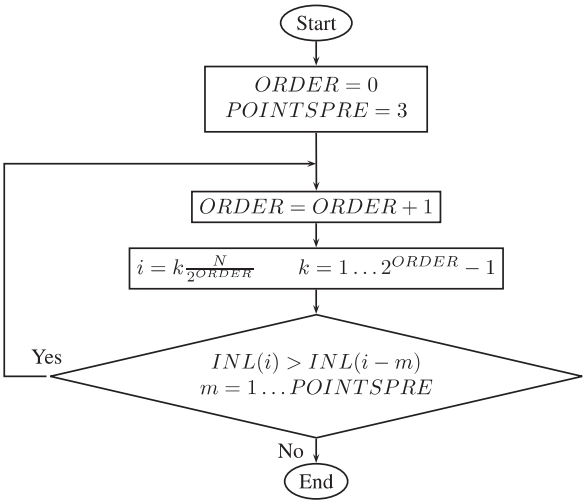

Fig. 1. Order finding.

2.2 *INL* Interpolation

Finding INL_{approx} vector is based on the Least Mean Squares (LMS) algorithm. The whole INL vector is separated into fractions with equal length. In Fig. 2, 3 and 4, these parts are marked as INL_p. The number of sections is calculated from the ORDER value. Every part is processed separately. Four times four points are selected from the INL_p and these values are interpolated by a first-order function (straight line). The LMS_x notation means Least Mean Square algorithm of x^{th} order. Data are selected near the quarters of the interval INL_p. There is a reason why the data are not taken exactly in the quarters. Specifically, there is a possibility that some higher order HCF artifacts remain in the data and this is the method how their importance can be suppressed. Sixteen points are selected because it is a good compromise between the compression and accuracy. It should be noted that this specific number was chosen for the best approximation of given data set with minimum number of measured points. In Fig. 4a), b) and c) the selection of sixteen points from INL_p is illustrated, their interpolation by the first order function (straight line) and whole INL_{approx} data are shown, respectively.

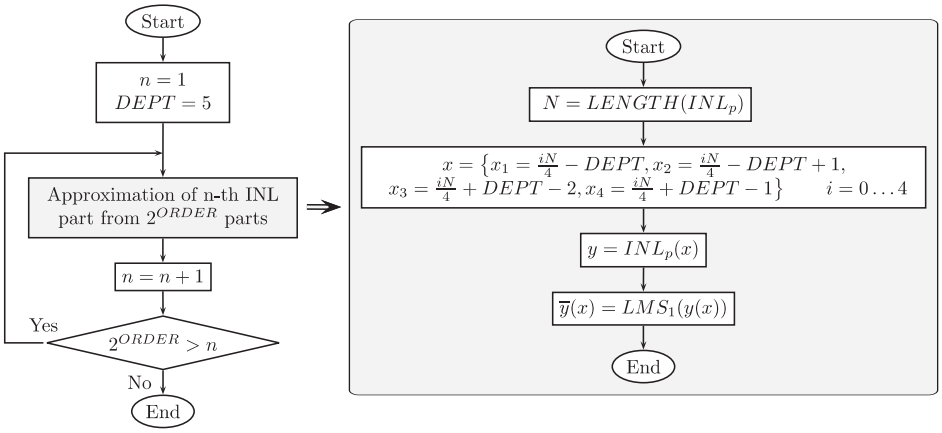

Fig. 2. INL_{approx} computing.

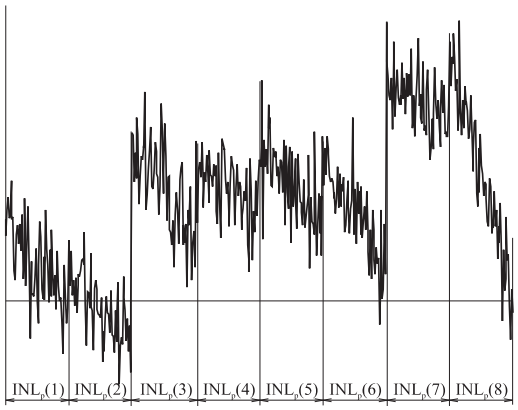

Fig. 3. INL data separation into parts.

2.3 Acquisition of LCF

The first task is to obtain the LCF component. This computation starts with LMS_1 interpolation of INL_{approx}. This interpolation is needed so as to find out the first and the last point (Fig. 6a). Other points are selected as arithmetical mean of lower and upper step value in INL_{approx} data (Fig. 6b). Based on the previous example, we calculate means at the border of all eight sections of INL_{approx}. These seven results, together with start and end points of LMS_1 approximation enter the LMS_4 algorithm. Output is the LCF component and its coefficients (Fig. 6c).

2.4 HCF Coefficients Calculation

The aim of the algorithm's last part is to find the HCF coefficients. At the procedure start, the matrix X is created. It contains zeros except at the positions corresponding to Rademacher function steps. Here, the row index in the matrix X corresponds to the Rademacher function order (see Fig. 7a). Based on X, the $XNEW$ matrix is calculated by logical inequality function (XOR) (Fig. 7b). Subsequently, the INL step size is obtained by multiplication of the $XNEW$ by INL_{Approx} differential (Fig. 7c). The average of step sizes corresponds to cumulative sum of Rademacher coefficients; note that inverse procedure is used for their calculation (Fig. 7d). HCF (Fig. 7f) is the difference between the cumulative sum of steps (Fig. 7e) and LMS_1 approximation of this sum.

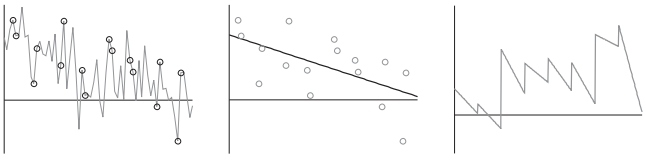

Fig. 4. Selection of sixteen points of INL_p a), interpolation of them b) and the whole INL_{approx} function c).

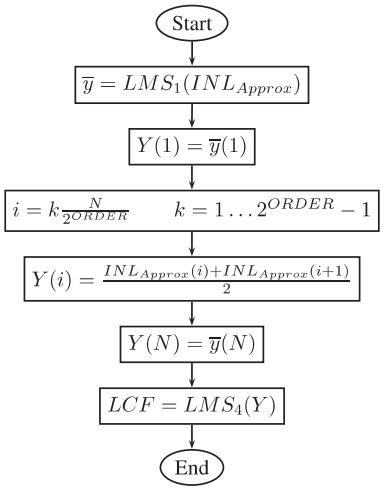

Fig. 5. LCF extraction flowchart.

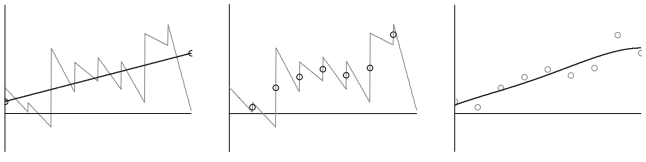

Fig. 6. LMS_1 interpolation of INL_{approx} a), arithmetical mean of lower and upper step value b) and LCF component c).

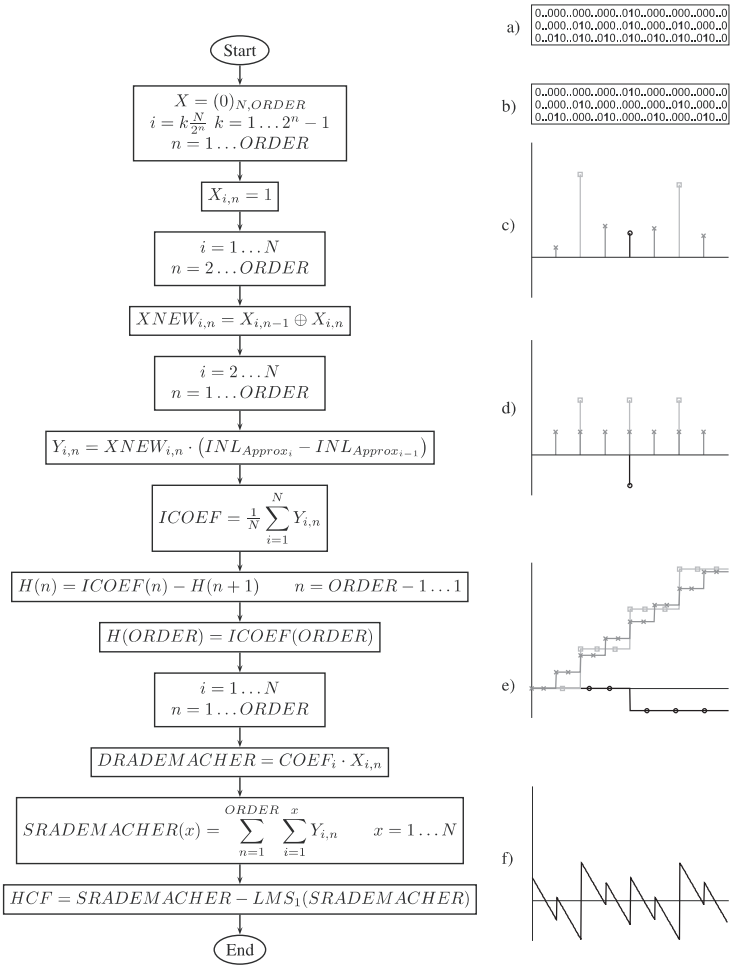

Fig. 7. HCF coefficients computing: Flowchart, a) X matrix, b) $XNEW$ matrix, c) $Y_{i,n}$ matrix, d) $DRADEMACHER$ matrix, e) $Y_{i,n}$ cumulative sum and f) HCF function.

3. Modeling Results

There is a modeling example in this Section. The architecture of the measured device is based on charge-redistribution successive approximation principle which is an implementation type of SAR ADC. These data were measured by ASICentrum company [12]. The HCF and LCF INL error model is very suitable for description of this kind of ADCs.

The result after INL fitting is shown in Fig. 8. Sampling frequency $f_s = 500$ kHz is within the Device Under Test (DUT) typical operating range. Therefore, we can take this situation as a 'static case'. Dominant error sources at this operating point are capacitance mismatch, comparator offset, etc. As it results from Tab. 1, our error model fits these data very well. This is apparent form the high value of the Model Coverage (MC) coefficient in the last column, see (6) for explanation. On the other hand, Fig. 9 shows the case where sampling frequency is too high ($f_s = 1200$ kHz) and where several relatively high peaks occur in the INL data. These peaks are not captured by the LCF and HCF functions in our point of view. In Tab. 1, the last row implies the low value of Model Coverage too.

The testing set [12] main part was a programmable DC power supply Agilent E3631A. The accuracy of INL data measurement was limited mainly by the properties of this source to 0.09 LSB.

The data in E_x rows of Tab. 1 represent the energy of the signal. It is computed in accordance with (5). The Model Coverage value is obtained by (6).

$$E_x = \frac{1}{N}\sum_{k=1}^{N} x^2(k), \tag{5}$$

$$MC = 1 - \frac{E_{INL-HCF-LCF}}{E_{INL}}. \tag{6}$$

Parameter	$f_s = 500$ kHz	$f_s = 1200$ kHz
E_{INL}	0.0120	0.221
$E_{INL-INL_{Approx}}$	0.0013	0.179
$E_{INL-HCF-LCF}$	0.0019	0.190
MC	0.600	0.072

Tab. 1. INL modeling efficiency.

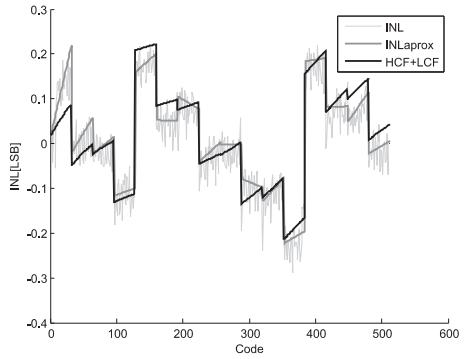

Fig. 8. SAR ADC INL modeling f_s = 500 kHz.

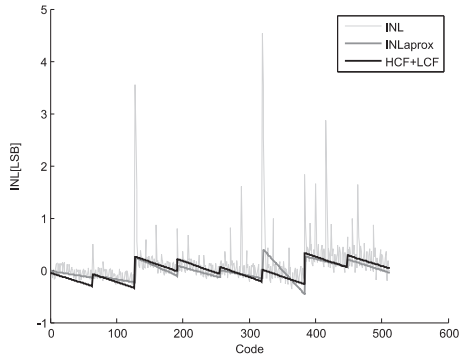

Fig. 9. SAR ADC INL modeling f_s = 1200 kHz.

Coefficient order n	L_n [LSB]	
	$f_s = 500$ kHz	$f_s = 1200$ kHz
0	$17.1 \cdot 10^{-3}$	$-118 \cdot 10^{-3}$
1	$1.67 \cdot 10^{-3}$	$0.788 \cdot 10^{-3}$
2	$-16.5 \cdot 10^{-6}$	$-1.59 \cdot 10^{-6}$
3	$47.1 \cdot 10^{-9}$	$0.212 \cdot 10^{-9}$
4	$-41.0 \cdot 10^{-12}$	$3.03 \cdot 10^{-12}$

Tab. 2. LCF coefficients.

Coefficient order n	H_n [LSB]	
	$f_s = 500$ kHz	$f_s = 1200$ kHz
1	-0.323	-0.462
2	0.343	0.369
3	0.115	0.231
4	-0.138	-

Tab. 3. HCF coefficients.

4. Conclusion

This article contains innovative INL fitting description. The most important novelty is a significantly reduced number of modeled points. This improvement is a great asset for the methodology used in ADC design, as it is predominantly oriented to IC design support tool. The algorithm was applied to real measured data set, the fitted model was shown in the figure and the model parameters were summarized in Tabs. 2 and 3. A very good performance of the model was documented by Model Coverage and Energy metrics in Tab. 1. Model limitations were also discussed.

Acknowledgements

The work was supported by the SGS grant No. OHK3-029/10, by the Grant Artemis JU No. 100029-SCALOPES and also by research program No. MSM 6840770014.

References

[1] BURNS, M., ROBERTS, G. W. *An Introduction to Mixed-Signal IC Test and Measurement*. New York (USA): Oxford University Press, 2001, p. 447 - 481.

[2] GRIMALDI, D., MICHAELI, L., MICHALKO, P. Identification of ADC error model by testing of chosen code bins. In *Proceedings of 12th IMEKO TC4 International Symposium*. Zagreb (Croatia), 2002.

[3] JUAN, P., HONG, M., CHEN, T. Modeling of ADC nonlinearity by time-delay-based power series. In *Second Asia International Conference on Modeling and Simulation*. Kuala Lumpur Malaysia, 2008, p. 1048 - 1053.

[4] HAASZ, V., SLEPIČKA, D., SUCHÁNEK, P. Models of the ADC transfer function - sensitivity to noise. In *IEEE International Instrumentation and Measurement Technology Conference*. Victoria (Canada), 2008, p. 583 - 587.

[5] BERNIERI, A., DAPONTE, P., GRIMALDI, D. ADC neural modeling. *IEEE Transactions on Instrumentation and Measurement*, 1996, vol. 45, no. 2.

[6] MICHAELI, L., SALIGA, J., MICHALKO, P. Triangular testing signal for identification of unified error model parameters. *Measurement Journal*, 2007, vol. 40, p. 491 - 499.

[7] MEDAWAR, S., BJÖRSELL, N., HÄNDEL, P., JANSSON, M. Dynamic characterization of analog-digital-converters non-linearities. In *Mosharaka International Conference on Wireless Communications and Mobile Computing*. Amman (Jordan), 2007.

[8] MEDAWAR, S., BJÖRSELL, N., HÄNDEL, P., JANSSON, M. Post-correction of pipelined analog–digital converters based on input-dependent integral nonlinearity modeling. *IEEE Transactions on Instrumentation and Measurement*, 2011, vol. 60, no. 10, p. 3342 - 3350.

[9] ŽIDEK, J., ŠUBRT, O., MARTINEK, P., Novel design evaluation engine for A/D converters. In *5th International Conference on Ph.D. Research in Microelectronics & Electronics, PRIME 2009*. Cork (Ireland), 2009, p. 240 - 243.

[10] ŽIDEK, J., ŠUBRT, O., MARTINEK, P. An innovative verification approach for nyquist-rate A/D converters - algorithm and implementation. *Electroscope*, 2009, vol. 11. [Online] Cited 2010-06-21. Available at: http://147.228.94.30/images/PDF/Rocnik2009/EDS_2009/zidek.pdf.

[11] RŮŽIČKA, Z. Walsh functions and the ways of their generation. *Elektrorevue*, 2004. [Online] Available at: http://www.elektrorevue.cz/clanky/04065/index.html, (in Czech).

[12] ASICentrum. *Measured Data Set of 9-bit SAR ADC*, 2010.

Jan ŽIDEK was born in Liberec on February 14, 1983. He received the Master degree (Ing.) from the Czech Technical University in Prague, faculty of Electrical Engineering (2008), where he has been studying a Ph.D. program

since that time. His research interests include novel design and verification methods of data converters. He completed a half-year internship at University of Limerick, Ireland (spring 2011).

Ondřej ŠUBRT was born in Hradec Králové on February 24, 1977. He works as senior IC designer with ASICentrum Prague, a company of the Swatch Group. He has also been appointed an Ass. Prof. at the Faculty of Electrical Engineering CTU Prague. His research interests being analog and mixed-signal integrated circuits design with emphasis to low-power low-voltage techniques and novel design and verification methods of data converters.

Milan VALENTA was born in Prostějov on March 30, 1983. He graduated (Master degree) in January 2008 at the Czech Technical University (CTU) in Prague, Faculty of Electrical Engineering and (Bachelor degree) in January 2010 at Charles University in Prague, Faculty of Mathematics and Physics. The master thesis (CTU) was focused on analysis and design of current-mode functional blocks. After master graduation in 2008 he started with Ph.D. studies at CTU. He completed a half-year internship (fall 2008) at Friedrich-Alexander University in Erlangen, Germany. In 2011 he joined ON Semiconductor and has worked as a design engineer.

Pravoslav MARTINEK was born in Ústí nad Labem on September 6, 1936. He received the Electrical engineering degree (Ing.) and PhD (CSc.) degree from the Czech Technical University in Prague, faculty of Electrical Engineering in 1967 and 1974 respectively. In 1968 he joined the Department of Circuit Theory at CTU and has been an Associate Professor since 1984. His primary research interest is analog signal processing, continuous- and discrete-time analog filters and current-mode electronic circuits.